Sub-Retinal Pigment Epithelial Deposits in a Dominant Late-Onset Retinal Degeneration

Christopher A. Kuntz, Samuel G. Jacobson,†‡ Artur V. Cideciyan,†‡ Zong-Yi Li,* Edwin M. Stone,§ Daniel Possin,* and Ann H. Milam**

Purpose. To determine the pathogenesis of an autosomal dominant late-onset retinal degeneration by studies of the retinal histopathology, phenotype of family members, and candidate genes for the disease.

Methods. The retina from an 80-year-old patient donor was prepared for light and electron microscopy, including special stains and immunocytochemistry. Family members were examined clinically and with retinal function tests. Rhodopsin, peripherin/*RDS*, and *TIMP3* genes were screened for mutations, and linkage analysis was performed with short tandem repeat polymorphisms flanking these genes.

Results. Affected family members had nyctalopia in the sixth decade of life and severe visual loss developed by the eighth decade. The donor retina showed marked loss of photoreceptors except in the inferior periphery. A thick layer of extracellular deposits was present between the RPE and Bruch's membrane in all retinal regions. A 70-year-old affected family member had a retinopathy resembling retinitis pigmentosa. Her 42-year-old daughter had a patch of punctate yellow–white lesions in one fundus and abnormal dark adaptation. The 50-year-old son of the donor had normal fundi but abnormal dark adaptation and electroretinography. No mutations were detected in the coding sequence of the rhodopsin, peripherin/*RDS*, and *TIMP3* genes. Rhodopsin and *TIMP3* were further excluded with linkage analysis.

Conclusions. This novel retinal degeneration shares histopathologic and clinical features with both Sorsby fundus dystrophy and retinitis pigmentosa. The sub-RPE deposits may disrupt the exchange of nutrients and metabolites between the retina and the choriocapillaris, leading to photoreceptor dysfunction and degeneration. Invest Ophthalmol Vis Sci. 1996;37:1772–1782.

Deposits between the retinal pigment epithelium (RPE) and Bruch's membrane are characteristic of age-related macular degeneration (ARMD)[1] and Sorsby fundus dystrophy (SFD).[2] It has been hypothesized[3,4] that such sub-RPE deposits may disrupt transport processes between the choriocapillaris and photoreceptors and lead to loss of vision.

We obtained the eyes of a patient donor from a family with an autosomal dominant (ad) late-onset retinal degeneration resembling retinitis pigmentosa (RP). Our histopathologic examination revealed a thick layer of deposits between the RPE and Bruch's membrane. A detailed light and electron microscopic study was performed, including special stains and immunocytochemistry, to characterize the sub-RPE deposits. Other family members were examined clinically and with visual function tests to determine the pattern of disease expression. Molecular genetic studies were performed to determine whether rhodopsin or peripherin/*RDS*, candidate genes for RP, or the *TIMP3* gene, recently found to cause SFD,[5] were responsible for this retinal degeneration.

METHODS

Subjects

Subjects were from a family whose history included three generations affected with blindness in later life

*From the *Department of Ophthalmology, University of Washington, Seattle; the †Scheie Eye Institute, University of Pennsylvania, Philadelphia; the ‡Bascom Palmer Eye Institute, University of Miami; and the §Department of Ophthalmology, University of Iowa, Iowa City.*

Supported by The Foundation Fighting Blindness (Baltimore, MD), The Chatlos Foundation, Inc. (Longwood, FL), Research to Prevent Blindness, Inc. (New York, NY), the Carver Charitable Trust; the Grousbeck Family Foundation, and by NIH Grants EY01311 and EY01730 (AHM); EY05627 (SGJ), and EY10539 (EMS).

Submitted for publication February 5, 1996; revised April 3, 1996; accepted May 2, 1996.

Proprietary interest category: N.

Reprint requests: Ann H. Milam, Department of Ophthalmology, University of Washington, Box 356485, Seattle WA 98195-6485.

Investigative Ophthalmology & Visual Science, August 1996, Vol. 37, No. 9

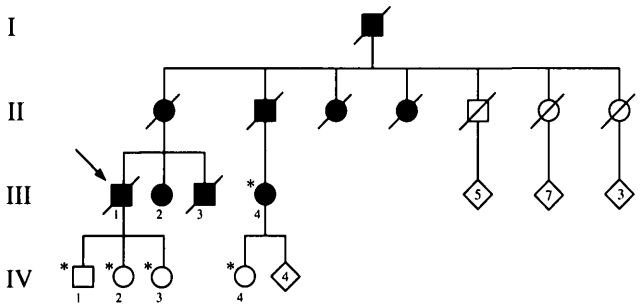

FIGURE 1. Pedigree of the family with late-onset retinal degeneration. Filled symbols represent family members with blindness; hatching indicates two generation IV members with abnormal fundus appearance, visual function test results, or both. Persons who underwent eye examinations and retinal function tests in this study are indicated by (*). Slashed symbols represent deceased members. Arrow indicates patient donor.

(Fig. 1). Medical records were obtained for the patient donor and an affected sister. The three children of the donor and two other family members underwent an ocular examination and visual function tests as part of the current study. Informed consent was obtained from the patients and from normal subjects after the nature of the procedures had been fully explained. Research procedures were in accordance with institutional guidelines and the Declaration of Helsinki.

Histopathology

The patient died of myocardial infarction at 80 years of age, and his eyes were fixed at 5 hours postmortem through the donor program of The Foundation Fighting Blindness (donation #356). The right eye was fixed in phosphate-buffered 4% paraformaldehyde and 0.5% glutaraldehyde; the left eye was frozen at −80°C and later thawed in the same fixative for gross pathology study. Tissue samples were embedded in paraffin, sectioned at 8 to 12 μm, and processed with special stains: Masson and Gomori trichrome, periodic acid-Schiff (PAS), Von Kossa, Alizarin Red, Perls, rubeanic acid, and Alcian blue at magnesium chloride concentrations of 0.06 to 0.9 M. Cryosections (12 μm) of the retina were processed with lipid stains (Oil Red O; Sudan Black B), for indirect immunofluorescence[6] using Cy3-labeled secondary antibodies, and for immunocytochemistry using the avidin–biotin peroxidase complex technique (Vector Elite Kit; Vector Labs, Burlingame, CA). Other retinal samples were post-fixed in phosphate buffered 1% OsO_4, embedded in Medcast, and processed for transmission electron microscopy.[6] Nonosmicated samples of retina were embedded in LR White resin and processed for electron microscopic immunocytochemistry using 5 nm gold-labeled secondary antibodies with silver intensification. Control sections for immunofluorescence, avidin–biotin peroxidase complex immunocytochemistry, and immunogold labeling were processed in the same manner with nonimmune primary antibody or with secondary antibody alone.

The following antibodies were used for immunocytochemistry: anti-amyloid P (1:50; from Dr. M. Skinner, Boston University, Boston, MA); anti-cellular retinaldehyde-binding protein (CRALBP, 1:100; from Dr. J. Saari, University of Washington, Seattle); anti-glial fibrillary acid protein (GFAP, 1:100; Dako, Carpinteria, CA); anti-rhodopsin (4D2 and 1D4, 1:40; from Dr. R. Molday, University of British Columbia, Vancouver); anti-elastin (1:50; Elastin Products, Owensville, MO); anti-lysozyme (1:100; BioGenex, San Ramon, CA); anti-fibronectin (1:10; Calbiochem, San Diego, CA); and anti-heparin sulfate proteoglycan (HSPG; 1:10; Chemicon, Temecula, CA).

Visual Function Tests

Dark adaptometry was performed in the subjects with good visual acuity (patients IV-1 to IV-4; Table 1) using

TABLE 1. Clinical Characteristics and Electroretinography Results

			Rod ERG		*Mixed Cone-Rod ERG†*		*Cone ERG*			
							1 Hz		*29 Hz*	
Patient	*Age (years)/Sex*	*Visual Acuity**	*Amp (μV)*	*Timing (msec)*	*B-wave (μV)*	*A-wave (μV)*	*Amp (μV)*	*Timing (msec)*	*Amp (μV)*	*Timing (msec)*
III-4	75/F	HM‡	ND§	ND	ND	ND	ND	ND	5	37.8
IV-1	49/M	20/20	128	88.8	391	281	168	31.2	159	29.2
IV-2	47/F	20/20	227	85.6	484	320	187	33.2	160	28.2
IV-4	42/F	20/20	248	82.0	313	242	204	30.8	193	31.2
IV-3	40/F	20/20	219	84.0	527	324	259	30.0	195	27.6
Normal										
Mean			299	76	497	297	173	33	172	30
(SD)			(52)	(5)	(111)	(65)	(32)	(1.3)	(35)	(1.2)

* Same in both eyes; † amplitudes; ‡ hand movement at 1 foot; § nondetectable.
ERG = electroretinogram; F = female; M = male.

a modified automated perimeter and techniques previously described.[7] In brief, prebleach thresholds were determined after >3 hours of dark adaptation. The recovery of sensitivity after a 7.8 log scot·td·s retinal exposure of yellow light, expected to bleach approximately 99% of the rhodopsin present, was measured with 500 nm and 650 nm stimuli (1.7° in diameter) at a test locus 30° in the nasal field. For a patient without central fixation (III-4), adaptometry was performed under visualization of the fundus using an automated imaging dark adaptometer.[8] The test locus was determined by performing thresholds within this patient's temporal retinal region of vision and measuring adaptation at the location of best threshold (an eccentricity of approximately 30°) with a white stimulus (diameter, 1.7°). This stimulus is 16 dB brighter in scotopic units than the 500 nm stimulus. Full-field electroretinography was performed with a computer-based system and a standard protocol previously described.[7]

DNA Analysis

Blood samples were obtained from family members known to be affected, including the patient donor, his affected sister, and an affected first cousin. Samples also were obtained from family members (generation IV) who had a 50/50 chance of inheriting the disease. The coding sequences of the rhodopsin, peripherin/*RDS*, and *TIMP3* genes were screened for mutations. Primers for STRP markers (IL2RB, D22S283, ACPP, RDS) were provided by the Cooperative Human Linkage Center, University of Iowa, or Research Genetics (Huntsville, AL), and patients were genotyped at these loci.

RESULTS

Patient Donor: Case Report

The patient donor had no visual complaints until he began to experience night vision disturbances at age 56. Medical records of examinations at another institution at ages 58, 59, and 65 were available. At age 58, he had 20/20 visual acuity but a delayed time course of dark adaptation. Electroretinographic testing revealed severely reduced rod b-wave amplitudes, reduced a- and b-waves to a maximal white stimulus in the dark, and borderline abnormal cone electroretinograms (ERGs). Ophthalmoscopy showed punctate yellow–white lesions in one eye. Fluorescein angiography revealed "several hyperfluorescent areas compatible with a fairly diffuse abnormality of the pigment epithelium." At age 59, visual acuity remained at 20/20, but a repeat ERG in the same laboratory showed no detectable rod b-wave and lower amplitudes to the maximal stimulus and to the cone ERG than on the previous recording. The patient had pro-

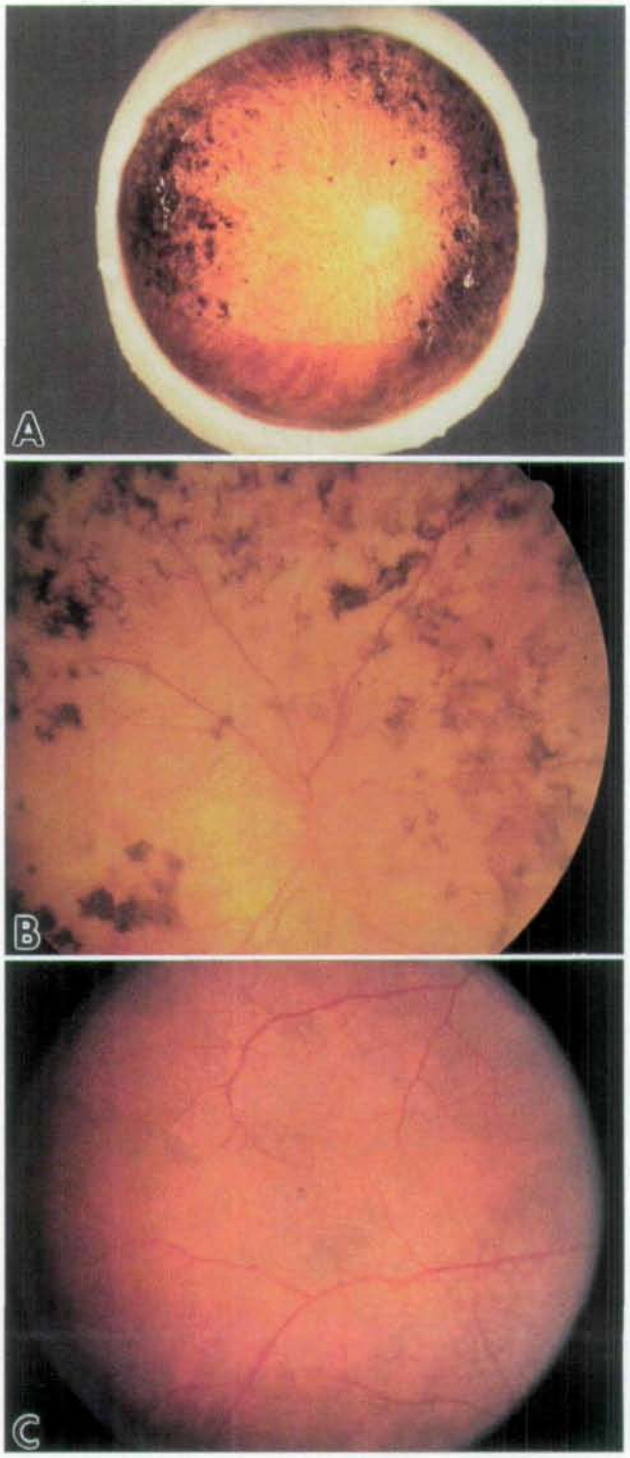

FIGURE 2. (**A**) Gross pathology of the right eye of the patient donor. Note bone spicule-like pigmentation in the superior, temporal, and nasal portions of the retina. There is a sharp line of demarcation in the inferior retina between the degenerated superior retina and the more normal-appearing inferior peripheral retina. (**B**) Fundus photograph of the right eye of patient III-4 showing bone spicule-like pigment and atrophy throughout the fundus. (**C**) Fundus photograph of the right eye of patient IV-4, which has a normal fundus appearance except for a patch of yellow–white punctate lesions in the temporal midperiphery.

gressive loss of vision, and, at age 65, visual acuity was 1/200, there were large central scotomas, and ERGs were not detectable. He was diagnosed with RP.

Patient Donor: Retinal Histopathology

Gross Pathology. The corneas, anterior segments, and vitreous were normal, but both lenses had small anterior and posterior cortical cataracts. The optic nerves were pale and atrophic, and the retinal vessels were attenuated. The retinas had bone spicule-like pigmentation from the midperiphery to far periphery in the temporal, superior, and nasal regions (Fig. 2A). Each eye had a sharp, horizontal line in the inferior midperipheral retina that separated the grossly abnormal retina from normal-appearing retina in the inferior far periphery. The larger choroidal vessels were visible as a consequence of degenerative changes in the RPE.

Microscopic Pathology (Right Eye). The optic nerve was severely atrophic with loss of normal axonal columns, reactive gliosis, and narrowing of the central retinal vessels. The superior, nasal, and temporal retinal regions, including the macula, showed total loss of photoreceptors, with atrophy and reactive gliosis of the inner retinal layers. Bone spicule-like pigmentation, characteristic of RP,[9] was scattered throughout these regions. Inferiorly, an abrupt transition from diseased to normal-appearing retina corresponded to the horizontal line observed grossly. Just superior to this line, the RPE, choriocapillaris, and photoreceptors were absent, and the inner retina was gliotic (Figs. 3A). Inferior to this line, the RPE, choriocapillaris, rod and cone photoreceptors, and inner retinal layers were intact, although there was focal loss of photoreceptor nuclei (Fig. 3B).

A confluent layer of PAS (+) extracellular material was present between the RPE and Bruch's membrane (Figs. 3A, 3B, 3C). This layer had variable thickness and terminated anteriorly at the ora serrata and posteriorly at the edge of Bruch's membrane at the optic nerve head. In the degenerated retinal regions, the sub-RPE layer of deposits was 50 μm or thicker, whereas in the inferior retina, it was thinner than 50 μm. The layer was generally acellular, but occasional melanin-containing RPE cells were noted within the deposit (Fig. 3A), particularly in the inferior retina just superior to the horizontal line. Empty-appearing lacunae appeared to be left in the deposit after loss of the entrapped RPE cells (Fig. 3A). Sub-RPE neovascularization was prominent in the degenerated retinal regions (Figs. 3C, 4A), and a large disciform scar was present in the region of the macula.

The outer half of the sub-RPE deposit was positive with Oil Red O (Fig. 3D) and Sudan Black B lipid stains, particularly in the inferior far peripheral retina where the RPE was retained in situ. The inner half of the deposit showed weak to absent lipid staining. The Von Kossa and Alizarin Red methods for calcium and the Perls method for iron stained clumps of crystalline material within the deposit. The rubeanic acid stain for copper was negative.

With the Masson and Gomori Trichrome stains, the deposit was positive for collagen throughout, particularly the inner sublayer. The retina was stained red with the Masson procedure, as were the lacunae in the sub-RPE deposits left after loss of entrapped RPE cells (Fig. 3E). With Alcian blue for sulfated mucosubstances, the inner sublayer was positive at all concentrations of magnesium chloride tested (0.06 to 0.9 M), but the outer sublayer was Alcian blue negative.

Light Microscopic Immunocytochemistry. The RPE and Müller cells were positive with anti-CRALBP in all regions of the retina. In the far inferior retina, anti-GFAP labeling was intense in the astrocytes and weak in the Müller cell radial processes. In the retinal regions where the RPE and photoreceptors had been lost, anti-GFAP labeled the hypertrophied Müller cells (Figs. 3F, 3G). Processes of the Müller cells formed whorls within the deposits that were labeled with both anti-CRALBP and anti-GFAP. These whorls filled the lacunae in the deposits (Figs. 3F, 3G, 5A).

Rod outer segments and somata in the inferior far periphery (Fig. 3H) were strongly labeled with anti-rhodopsin. Long, rhodopsin-positive neurites that originated from these rod somata[10] coursed along the hypertrophied Müller processes that filled the areas of lost photoreceptors and RPE cells, terminating as whorls in the lacunae that contained Müller cell processes (Fig. 3H). The rod neurites extended from the rod somata to the degenerate superior retina, in some cases for several millimeters, before terminating on whorls of Müller processes in the deposits (not shown).

The outer half of the deposit was well labeled with anti-amyloid P and anti-lysozyme, especially in the inferior retina, where the RPE was retained in situ. The inner sublayer of the deposit was weakly positive with anti-elastin. Blood vessels in the retina and choroid were labeled with anti-fibronectin and anti-HSPG, but the layer of deposits was negative.

Control sections for immunofluorescence that had been treated with nonimmune primary antibody or with Cy3-labeled secondary alone showed weak autofluorescence of the sub-RPE deposit and neurons in the retina. Control sections for avidin–biotin peroxidase complex immunocytochemistry showed very weak, nonspecific background reaction.

Transmission Electron Microscopy. The layer of deposits was located between the basal lamina of the RPE and the inner collagenous layer of Bruch's membrane and consisted of heterogeneous materials of varying electron density. Three sublayers could be identified; an outer, foamy-appearing zone corre-

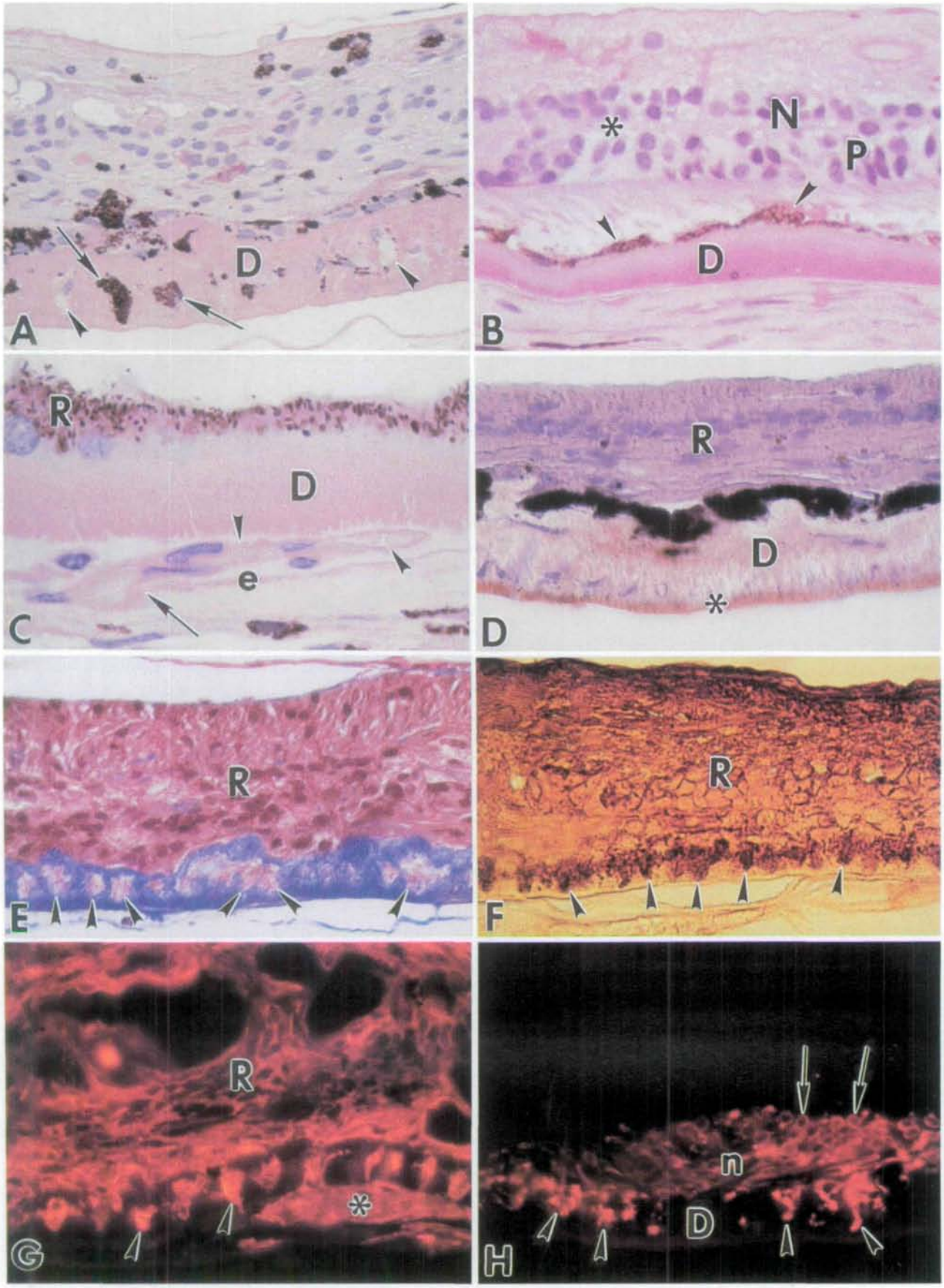

FIGURE 3. (**A**) Light microscopy of the degenerated, superior retina where photoreceptors are absent. The PAS (+) sub-RPE deposit (D) contains entrapped melanin-containing RPE cells (*arrows*) and lucent lacunae (*arrowheads*). Magnification, ×300. (**B**) The inferior retina has retained photoreceptors, but their nuclei are focally absent (beneath the *) and a thick PAS (+) layer (D) is present beneath the flattened RPE cells (*arrowheads*). RPE = retinal pigment epithelial cells; P = photoreceptor layer; N = inner nuclear layer. Magnification, ×400. (**C**) Light microscopy of Bruch's membrane illustrating a new vessel (*arrowheads*) that has passed through a break (*arrow*) in the elastin layer (e) of Bruch's membrane; R = retinal pigment epithelium; D = PAS (+) sub-RPE deposits. Magnification, ×500. (**D**) Cryosection of degenerated superior retina stained with Oil Red O, demonstrating lipid in the outer sublamina (*) of the sub-RPE deposit (D). R = gliotic retina. Magnification, ×400. (**E**) Paraffin section stained by Masson trichrome, demonstrating presence of collagen (stained blue) in the sub-RPE deposit. The gliotic retina (R) is stained red, as are Müller cell processes (*arrowheads*) that occupy lacunae within the sub-RPE deposits. Magnification, ×300. (**F**) Immunolabeling of degenerated retina by the avidin–biotin peroxidase complex method using anti-glial fibrillary acid protein (GFAP). Note strong labeling of hypertrophied Müller cells in the degenerated retina (R) and regularly spaced whorls of GFAP-positive Müller cell processes within lacunae (*arrowheads*) in the layer of deposits. Magnification, ×300. (**G**) Immunofluorescence with anti-GFAP in the superior retina, illustrating GFAP (+) Müller processes in degenerate retina (R) and within lacunae (*arrowheads*) in the otherwise unlabeled layer of deposits. A disciform scar (*) is GFAP (+). Magnification, ×400. (**H**) Immunofluorescence with anti-rhodopsin of inferior portion of the retina. Note labeling of the remaining rod somata (*arrows*) and rod neurites (n), which terminate in lacunae (*arrowheads*) within the otherwise unlabeled layer of deposits (D). Magnification, ×400

sponded to the layer positive for lipids (Figs. 4A, 4B, 5A). Lucent, chipped-out areas within the deposits corresponded to the inclusions that were positive with the calcium and iron stains (Fig. 5A). The inner sublayer, corresponding to the deposits that were positive by the Trichrome and Alcian blue stains, contained radiating frond-like structures of varying densities (Figs. 4, 5). Neovascularization was evident, with fenestrated capillaries present between the elastin layer of Bruch's membrane and the RPE (Fig. 4A).

Electron Microscopic Immunocytochemistry. Müller cell processes that filled lacunae in the deposit were labeled with anti-GFAP (Fig. 5B). Electron-dense amorphous deposits in the inner sublayer were positive with anti-elastin (Fig. 5C), in addition to the elastin surrounding the choroidal vessels and in Bruch's membrane. Control sections treated with nonimmune primary antibody or with gold-labeled secondary antibody alone had only a few, randomly scattered gold particles.

Family Members of the Patient Donor: Clinical and Visual Function Studies

A family historian recalled that most affected members first became symptomatic with night vision disturbances between 50 and 60 years of age and then experienced progressive loss of central and peripheral vision. Medical records were available for the patient donor's sister (patient III-2), who had been examined at other institutions. She had initial night vision complaints in her 50s but no visual acuity problems. On examination at age 61, she was diagnosed with "generalized primary choroidal degeneration." At age 63, her visual acuity was 20/20; kinetic perimetry (target, III-4e) revealed an extensive central scotoma of at least 60° with a small region at fixation that was preserved; color vision with a Farnsworth D-15 panel indicated a tritan axis of confusion; and ERGs were reduced in amplitude for rod and cone stimuli. The central retina was described as showing "an unusual degenerative change with irregular areas of pigment." The diagnoses given at this examination were "central and retinal degeneration, type unknown" or "SFD." Subsequently, there was loss of central and peripheral vision, and now, at age 88, the patient states she is "totally blind."

Table 1 lists the five patients who were examined in this study. Patient III-4, a 75-year-old affected family member, had normal vision until age 50, when she experienced onset of night vision problems; loss of central and peripheral vision occurred thereafter. On our examination, visual acuity was hand motion at 1 foot, and kinetic perimetry with the V-4e target revealed only a residual island in the nasal field of each eye. Ophthalmoscopy showed attenuated retinal vessels, bone spicule-like pigment, and chorioretinal atrophy throughout the fundus (Fig. 2B).

Four family members (40 to 49 years of age) in generation IV with a 50/50 chance of inheriting the disease also were examined. All had no visual symptoms, visual acuity of 20/20, full kinetic visual fields, and no color vision abnormalities with a Farnsworth D-15 panel. Two of the four individuals (patients IV-1 and IV-4) had fun-

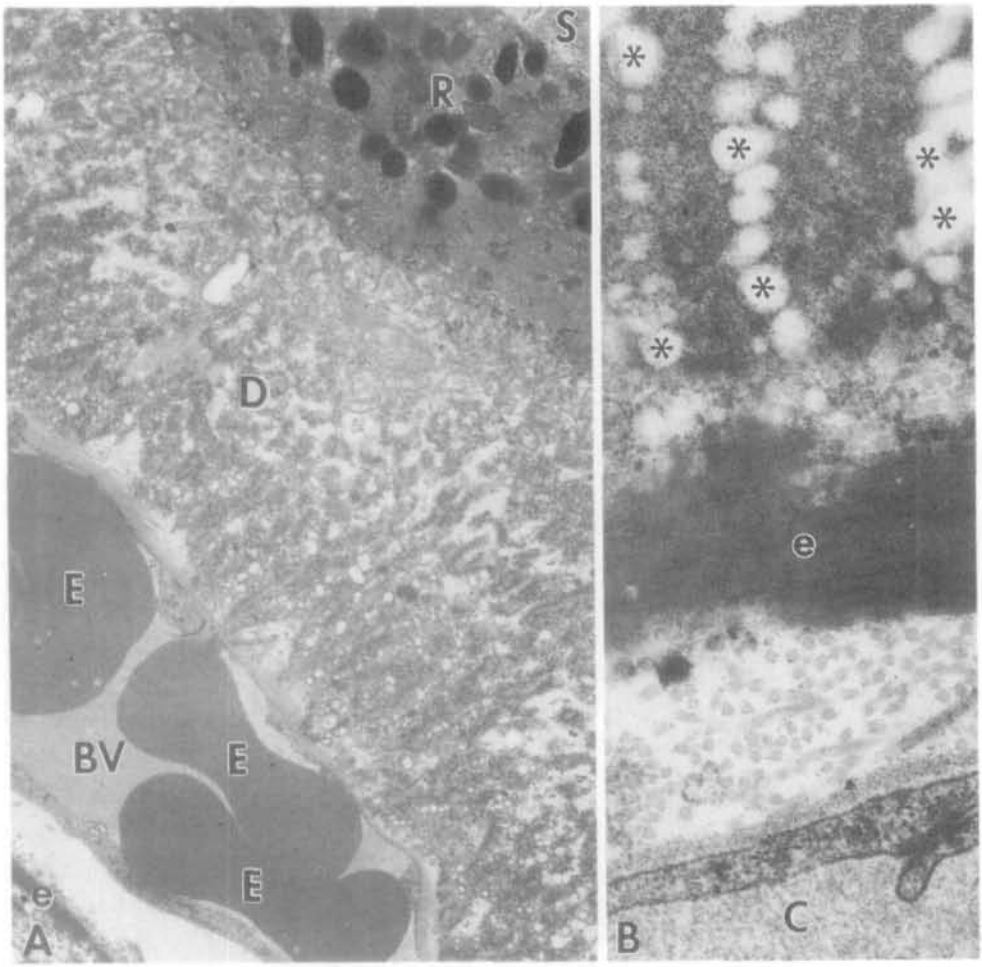

FIGURE 4. Transmission electron microscopy of sub-RPE deposits (D). (A) A thin-walled blood vessel (BV) derived from the choriocapillaris is present between the sub-RPE deposits (D) and the elastin layer (e) of Bruch's membrane. R = retinal pigment epithelium; S = subretinal space; E = erythrocytes. Magnification, ×5800. (B) Empty spaces (*) in the outer sublayer of the deposit reflect extraction of lipid during processing. e = elastin layer of Bruch's membrane; C = choriocapillaris. Magnification, ×42,580.

duscopic and/or visual function findings that suggested inheritance of the disease. Patient IV-1 had a normal fundus examination in both eyes, but patient IV-4 had a patch of yellow–white punctate lesions in the temporal and inferior midperipheral retina of the right eye (Fig. 2C).

Electroretinograms were normal in patients IV-2, IV-3, and IV-4. Patient IV-1 had an abnormal rod ERG b-wave, but all other waveforms were within normal limits. Patient III-4 had no detectable ERGs to all stimuli except cone flicker, which showed a severely reduced and delayed response (Table 1, Fig. 6). Dark adaptometry was normal for rods and cones in patients IV-2 and IV-3 but abnormal in patients III-4, IV-1, and IV-4 (Fig. 6). Patient III-4 had a final dark-adapted threshold that was elevated by almost 4 log units and a markedly delayed time course of adaptation. Patients IV-1 and IV-4 had normal final rod thresholds, but the time course of adaptation was abnormal. The rod–cone break was prolonged, and the time to reach final dark-adapted rod threshold was delayed. Cone thresholds at the plateau of the dark adaptation function were normal or nearly normal in patients IV-1 and IV-4, but the kinetics were abnormal.

DNA Analysis

Affected individuals in the family showed no mutations in the rhodopsin, peripherin/*RDS*, and *TIMP3* genes. In addition, short tandem repeat polymorphisms near these three genes were genotyped in the family. Recombination events were observed with markers IL2RB and D22S283 (markers near the *TIMP3* gene) and ACPP (marker near the rhodopsin gene). All markers tested in the vicinity of the peripherin/*RDS* gene were uninformative.

DISCUSSION

This ad late-onset retinopathy shares certain features with other well-known retinal degenerative diseases but shows sufficient differences to be considered a novel disease entity. Standard assays for mutations in the coding sequences of three candidate genes (rhodopsin, peripherin/*RDS*, and *TIMP3*) did not reveal any changes in the affected family members. The observation of recombination between the disease phenotype and markers near the rhodopsin and *TIMP3* genes makes it unlikely that either of these genes is involved in the patho-

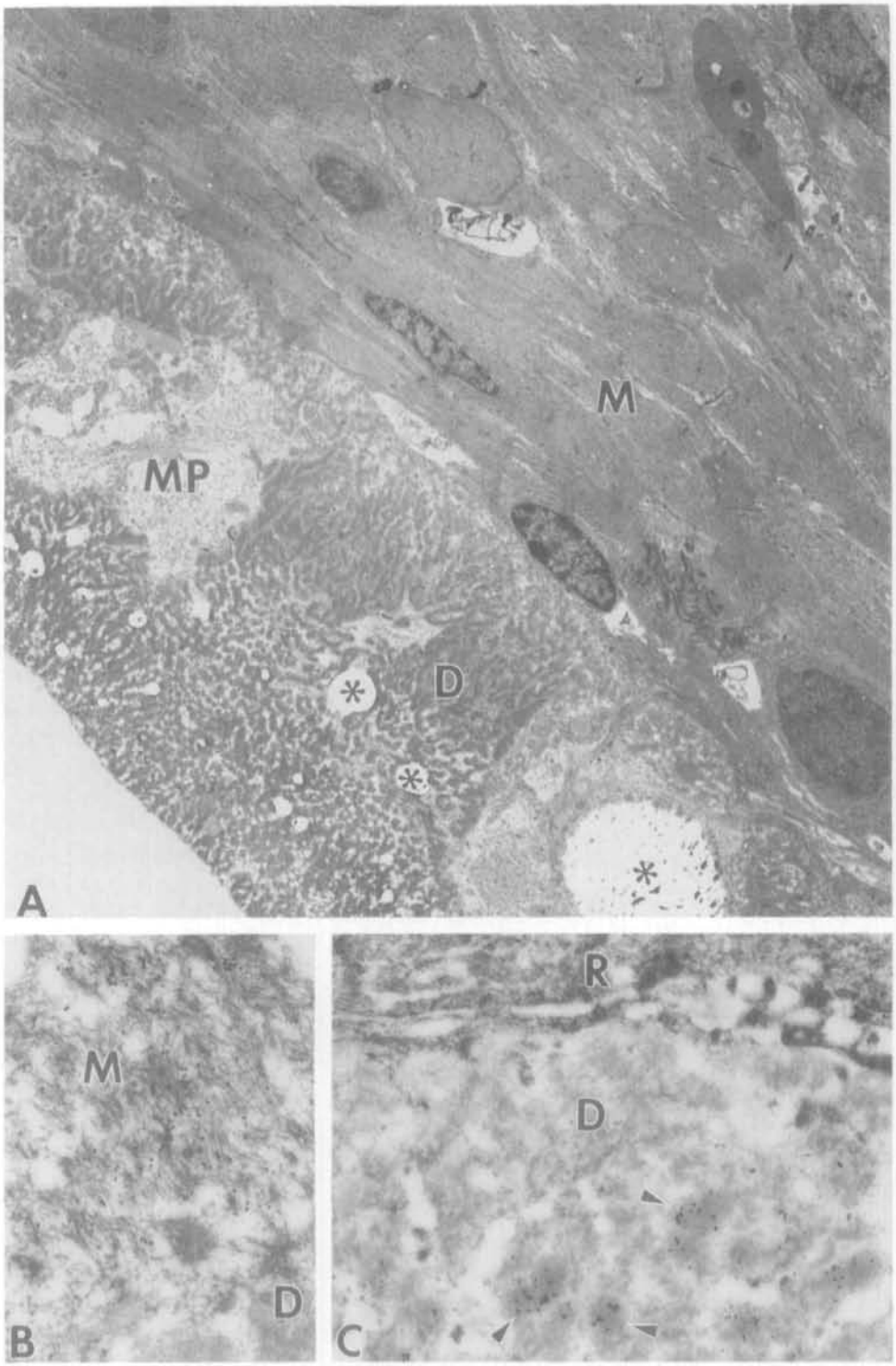

FIGURE 5. Transmission electron microscopy of sub-retinal pigment epithelial (RPE) deposits (D). (**A**) The superior retina lacks photoreceptors and RPE cells and is gliotic with hyperplasia of Müller cell processes (M). The chipped out areas (*) in the deposits (D) correspond to the calcium and iron-positive inclusions demonstrated by special stains. A lacuna in the deposit is filled with whorls of Müller cell processes (MP). The choroid has artifactually detached from the extracellular deposits. Magnification, ×2770. (**B**) Immunogold labeling with anti-glial fibrillary acid protein (GFAP). Note labeling of filaments in Müller processes (M) that fill a lacuna in the sub-RPE deposit (D). Magnification, ×29,000. (**C**) Immunogold labeling with anti-elastin. Note labeling of dense inclusions (*arrowheads*) in the sub-RPE deposit (**D**) near the RPE cell (R). Magnification, ×19,300.

genesis of the retinal degeneration in this family. Although no mutations were detected in the coding sequence of the peripherin/*RDS* genes of affected family members, this gene could not be further excluded with linkage analysis.

Clinically, the retinal disease described here does not lead to symptoms or ophthalmoscopic abnormalities until mid-life. The first symptoms are night vision problems, and the first funduscopic sign may be clusters of yellow–white punctate lesions. The earliest visual function abnormalities we found were a prolongation of dark adaptation in the 42- and 49-year-old family members and a reduction in the rod ERG b-wave in the 49-year-old member. Many forms of SFD, an ad retinopathy now known to be caused by mutations in the *TIMP3* gene,[5] tend to have an earlier onset of nyctalopia but can show a similar adaptation abnormality and eventual ERG amplitude reduction.[8,11] Of

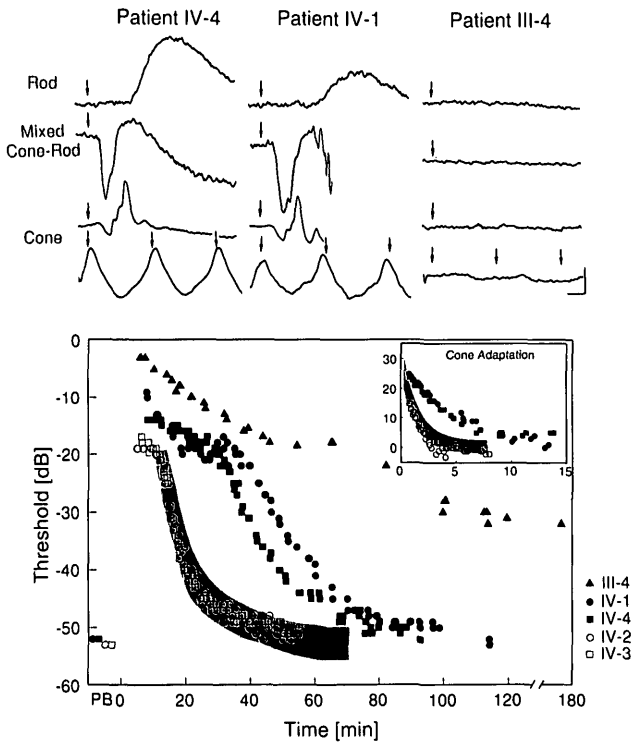

FIGURE 6. Visual function test results in family members of the patient donor. (**upper**) Rod, mixed cone-rod, and cone (1 Hz and 29 Hz) electroretinograms in patients IV-4, IV-1, and III-4. Arrows are at stimulus onset. Calibrations: vertically, 100 μV; horizontally, 20 msec for rod, mixed, and cone 1 Hz, but 10 msec for cone 29 Hz flicker. (**lower**) Dark adaptometry results in normal subjects and five patients after light exposure expected to bleach 99% of rhodopsin. Main graph shows data using a 500 nm stimulus for all patients except III-4, whose test was performed with a white stimulus; inset shows cone adaptation data using a 650 nm stimulus. Shading indicates range of normal results. PB = prebleach baseline dark-adapted thresholds. Data from patient III-4 have not been adjusted for the 16 dB difference between the white and the 500 nm stimuli.

course, patients with ad RP can have nyctalopia and ERG abnormalities, but it would be unusual for such patients to have normal eye examination results for decades before the onset of symptoms. Dark adaptation abnormalities have been described in ad RP patients with known and unknown genotypes,[7,12-15] but the pattern of adaptation in the family in this study, with marked prolongation of the rod-cone break and slow return to final threshold, is more similar to that in SFD and vitamin A deficiency[3,11,16] than in RP. Interestingly, some patients with ARMD, another late-onset retinopathy, can have problems with night vision and show this type of dark adaptation abnormality.[4]

Once the disease is manifest, progressive decline in visual function follows, with midperipheral scotomas, severe loss of central vision, and, finally, very limited visual perception. The advanced stages of the disease resemble severe RP with involvement of most of the retina and little or no detectable retinal function by ERG and psychophysical testing. We were unable to examine family members between early and late stages of the disease, so we are uncertain of the natural history of central vision loss. Scarring of the central retina in the 75-year-old patient could have been caused by choroidal neovascularization, subretinal hemorrhage, and macular degeneration as in SFD. However, this patient did not describe an acute loss of central vision, as is commonly noted by patients with SFD at the time of hemorrhagic macular degeneration.

A striking histopathologic feature of the donor retina was a thick layer of extracellular deposits between the RPE and Bruch's membrane. The deposit had two distinct sublayers: The outer one was rich in lipids and collagen and positive for amyloid P and lysozyme, and the inner sublayer contained collagen, mucosubstances, elastin, Müller processes, and rhodopsin-positive rod neurites. The deposit also contained calcium and iron. Except in the inferior periphery, there was marked loss of RPE and photoreceptor cells, choriocapillaris atrophy, and retinal gliosis. Choroidal neovascularization was prominent, including formation of a disciform macular scar. Although regional differences in severity of disease are not uncommon in RP,[17] this case had the unusual feature of a sharp horizontal line of demarcation between diseased and more normal-appearing retina in each eye.

Similar sub-RPE deposits have been noted in eyes from donors with SFD and dominant drusen. A 63-year-old patient with SFD had a thick, confluent layer of sub-RPE deposits, closely resembling those in this case, including sublayers that were PAS (+), stained for lipids (especially the outer sublamina), and contained calcium.[2] In dominant drusen, decreased acuity is noted in the fourth or fifth decade,[18] and yellow deposits are present in the posterior fundus. These deposits accumulate between the RPE and Bruch's membrane and are positive by PAS and Oil Red O stains. Extensive deposits in Bruch's membrane were found in three persons with late-onset retinal degeneration. Two brothers who had nyctalopia at ages 55 and 62 years had bone spicule-like pigment in the midperipheral retina and amorphous, thick deposits between the RPE and Bruch's membrane.[19] As in our case, the deposits were PAS (+) and had two sublayers, although the deposits were not examined for lipids or minerals. A woman with an ad retinal degeneration presented with nyctalopia at age 51.[20] Thick deposits were found between the RPE and Bruch's membrane that were PAS (+) and contained calcium. Electron microscopy revealed a frond-like pattern of the deposits, which had whorls of glial processes as found in our case.

Certain patterns emerge from the study of retinal

degenerations associated with deposits in Bruch's membrane. These disorders are often ad, and the patients are asymptomatic until adulthood. The deposits contain lipid and minerals, and the presumed secondary changes include dysfunction and loss of photoreceptors and RPE cells, choriocapillaris atrophy, choroidal neovascularization, and disciform scarring. Age-related macular degeneration (ARMD) resembles these retinal degenerations because of symptom onset in the fifth to sixth decade, drusen, sub-RPE deposits, choroidal neovascularization, and disciform scarring.[21] It is likely that disruption of the RPE–Bruch's membrane transport function contributes to the pathogenesis of ARMD.

Defects in the transfer of substances between the RPE and choriocapillaris, although possibly present from birth, may not become evident until the fifth or sixth decade of life. Interestingly, the hydraulic conductivity of Bruch's membrane drops strikingly with age in normal persons,[22] correlating with age-related accumulation of lipids in Bruch's membrane.[23] It is possible that Bruch's membrane has reserve permeability early in life and is able to compensate for some level of transport abnormality. Through the decades, normal aging changes in Bruch's membrane may result in reduced tolerance for defective transport. This hypothesis would explain the observation that patients with the disorders discussed above, including those with ARMD, have normal retinal function for decades and may even have normal results of fundus examination until late in life.

The thick sub-RPE deposits in the retina of the donor may reflect production by the RPE of an abnormal substance or an abnormal amount of a normal substance, or a defect in Bruch's membrane may make it less permeable to the normal products of RPE metabolism. Additional studies are needed on normal transport mechanisms in the RPE and Bruch's membrane to elucidate the pathophysiology of this important group of retinal diseases.

Key Words

retinal pigment epithelium, retinitis pigmentosa, Sorsby fundus dystrophy, TIMP-3

Acknowledgments

The authors thank Drs. F. W. Newell and R. E. Carr for assistance with the patient histories; Dr. R. E. Kalina for advice and critical review of the manuscript; Dr. S. Daiger for initial DNA screening; Ms. J. Glover–Kerkvliet for assistance with the tissue donation; Ms. K. Vandenburgh, Ms. J. Chang, and Ms. I. Klock for technical help; Mr. R. Jones and Mr. C. Stephens for photographic assistance; Mr. G. Regunath, Mr. Y. Huang, and Ms. J. Anderson for assistance with data acquisition and analyses; and Drs. J. Saari, R. Molday, and M. Skinner for providing antibodies. They also thank Mr. M. Benegas and Ms. K. Hummer for clinical coordination of this study.

References

1. Green WR, Enger C. Age-related macular degeneration histopathologic studies: The 1992 Lorenz E. Zimmerman Lecture. *Ophthalmology.* 1993;100:1519–1535.
2. Capon MR, Marshall H, Krafft JI, et al. Sorsby's fundus dystrophy: A light and electron microscopic study. *Ophthalmology.* 1989;96:1769–1777.
3. Steinmetz RL, Polkinghorne PC, Fitzke FW, et al. Abnormal dark adaptation and rhodopsin kintetics in Sorsby's fundus dystrophy. *Invest Ophthalmol Vis Sci.* 1992;33:1633–1636.
4. Steinmetz RL, Haimovici R, Jubb C, et al. Symptomatic abnormalities of dark adaptation in patients with age-related Bruch's membrane change. *Br J Ophthalmol.* 1993;77:549–554.
5. Weber BH, Vogt G, Pruett RC. Mutations in the tissue inhibitor of metalloproteinase-3 (*TIMP3*) in patients with Sorsby's fundus dystrophy. *Nature Genet.* 1994; 8:352–356.
6. Milam AH, Jacobson SG. Photoreceptor rosettes with blue cone opsin immunoreactivity in retinitis pigmentosa. *Ophthalmology.* 1990;97:1620–1631.
7. Jacobson SG, Kemp CM, Cideciyan AV, et al. Phenotypes of stop codon and splice site rhodopsin mutations causing retinitis pigmentosa. *Invest Ophthalmol Vis Sci.* 1994;35:2521–2534.
8. Azevedo DFG, Cideciyan AV, Regunath G, et al. An automated imaging dark adaptometer for investigating hereditary retinal degenerations. In: Parel J-M, Ren Q, Joos KM, eds. *Ophthalmic Technologies V.* Bellingham, WA: SPIE; 1995;2393:313–321.
9. Li Z-Y, Possin DE, Milam AH. Histopathology of bone spicule pigmentation in retinitis pigmentosa. *Ophthalmology.* 1995;102:805–816.
10. Li Z-Y, Kljavin IJ, Milam AH. Rod photoreceptor neurite sprouting in retinitis pigmentosa. *J Neurosci.* 1995;15:5429–5438.
11. Jacobson SG, Cideciyan AV, Regunath G, et al. Night blindness in Sorsby's fundus dystrophy reversed by vitamin A. *Nature Genet.* 1995;11:27–32.
12. Alexander KR, Fishman GA. Prolonged rod dark adaptation in retinitis pigmentosa. *Br J Ophthalmol.* 1984; 68:561–569.
13. Jacobson SG, Kemp CM, Sung C-H, et al. Retinal function and rhodopsin levels in autosomal dominant retinitis pigmentosa with rhodopsin mutations. *Am J Ophthalmol.* 1991;112:256–271.
14. Kemp CM, Jacobson SG, Roman AJ, et al. Abnormal rod dark adaptation in autosomal dominant retinitis pigmentosa with proline-23-histidine rhodopsin mutation. *Am J Ophthalmol.* 1992;113:165–174.
15. Moore AT, Fitzke FW, Kemp CM, et al. Abnormal dark adaptation kinetics in autosomal dominant sector retinitis pigmentosa due to rod opsin mutation. *Br J Ophthalmol.* 1992;76:465–469.
16. Kemp CM, Jacobson SG, Faulkner DJ, et al. Visual function and rhodopsin levels in humans with vitamin A deficiency. *Exp Eye Res.* 1988;46:185–197.

17. Li Z-Y, Jacobson SG, Milam AH. Autosomal dominant retinitis pigmentosa caused by the threonine-17-methionine rhodopsin mutation: Retinal histopathology and immunocytochemistry. *Exp Eye Res.* 1994;58:397–408.
18. Deutman AF. Macular dystrophies. In: Ryan S, ed. *Retina.* Vol. 2. St. Louis: CV Mosby; 1994:1186–1240.
19. Duvall J, McKechnie NM, Lee WR, et al. Extensive subretinal pigment epithelial deposit in two brothers suffering from dominant retinitis pigmentosa: A histopathological study. *Graefe's Arch Clin Exp Ophthalmol.* 1986;224:299–309.
20. Brosnahan DM, Kennedy SM, Converse CA, et al. Pathology of hereditary retinal degeneration associated with hypobetalipoproteinemia. *Ophthalmology.* 1994; 101:38–45.
21. Bressler NM, Bressler SB, Fine SL. Age-related macular degeneration. *Surv Ophthalmol.* 1988;32:375–413.
22. Moore DJ, Hussain AA, Marshall J. Age-related variation in the hydraulic conductivity of Bruch's membrane. *Invest Ophthalmol Vis Sci.* 1995;36:1290–1297.
23. Pauleikhoff D, Sheraidah G, Marshall J, et al. Biochemical and histochemical analysis of age related lipid deposits in Bruch's membrane. *Ophthalmologe.* 1994;91:730–734.